Carbohydrate Polymers 119 (2015) 118–125

Contents lists available at ScienceDirect

Carbohydrate Polymers

journal homepage: www.elsevier.com/locate/carbpol

Nanogels based on alginic aldehyde and gelatin by inverse miniemulsion technique: synthesis and characterization

P.R. Sarika [a], P.R. Anil Kumar [b], Deepa K. Raj [b], Nirmala Rachel James [a,*]

[a] Department of Chemistry, Indian Institute of Space Science and Technology (IIST), Valiamala, Thiruvananthapuram, Kerala 695 547, India
[b] Tissue Culture Laboratory, Biomedical Technology Wing, Sree Chitra Tirunal Institute for Medical Sciences and Technology, Poojappura, Thiruvananthapuram, Kerala 695 012, India

ARTICLE INFO

Article history:
Received 5 July 2014
Received in revised form
11 November 2014
Accepted 13 November 2014
Available online 24 November 2014

Keywords:
Alginic aldehyde
Gelatin
Inverse miniemulsion
Nanogels
Schiff's base reaction.

ABSTRACT

Nanogels were developed from alginic aldehyde and gelatin by an inverse miniemulsion technique. Stable inverse miniemulsions were prepared by sonication of noncontinuous aqueous phase (mixture of alginic aldehyde and gelatin) in a continuous organic phase (Span 20 dissolved in cyclohexane). Cross-linking occurred between alginic aldehyde (AA) and gelatin (gel) in the presence of borax by Schiff's base reaction during the formation of inverse miniemulsion. The effects of surfactant (Span 20) concentration, volume of the aqueous phase and AA/gel weight ratio on the size of the alginic aldehyde–gelatin (AA–gel) nanoparticles were studied. Nanogels were characterized by DLS, FT-IR spectroscopy, TGA, SEM and TEM. DLS, TEM and SEM studies demonstrated nanosize and spherical morphology of the nanogels. Hemocompatibility and *in vitro* cytocompatibility analyses of the nanogels proved their nontoxicity. The results indicated the potential of the present nanogel system as a candidate for drug- and gene-delivery applications.

1. Introduction

Nanosized hydrogel particles, also known as nanogels, formed from physically or chemically cross-linked polymer networks have bagged growing interest in recent years due to their unique features such as small size, large surface area, colloidal stability and high drug-loading capacity (Kabanov & Vinogradov, 2009; Raemdonck, Demeester, & De Smedt, 2009; Rejinold et al., 2012; Shah, Desai, Patel, & Singh, 2012). Nanogel particles have been developed by different approaches such as physical self-assembly, homogeneous or heterogeneous polymerization of monomers, cross-linking of preformed polymers, microfluidics, micromolding, photolithography, precipitation polymerization and inverse emulsion polymerization (Kabanov & Vinogradov, 2009; Oh, Drumright, Siegwart, & Matyjaszewski, 2008). An alternative, less energy-intensive method for the formation of nanogels is inverse miniemulsion. Nanomaterials such as polymeric nanoparticles, drug nanocrystals, semiconductors and magnetic particles have been prepared by this technique (Munshi, De, & Maitra, 1997; Nesamony & Kolling, 2005; Sato, Ohtsu, & Komasawa, 2000; Sims et al., 2002). Inverse miniemulsion can be obtained very easily by gentle mixing of appropriate amounts of water, oil and surfactant(s). The ease with which miniemulsion can be achieved makes it a preferred technique for nanoparticle synthesis. Spontaneously formed miniemulsions constitute of uniform-sized droplets or particles and possess narrow size distribution and spherical or near-spherical shape (Pileni, 1997).

Nanogels have been prepared from synthetic as well as natural polymers through different routes and their versatile applications have been illustrated (Daoud-Mahammed et al., 2009; Nesamony, Singh, Nada, Shah, & Kolling, 2012; Sasaki et al., 2011). Even though nanogels from synthetic polymers were investigated extensively, biopolymer-based nanogels assume significance due to their biodegradability, biological origin, abundance in nature, nontoxicity and the presence of large number of functional groups for possible conjugation with cell-targeting agents and drug molecules (Oh, Lee, & Park, 2009). Among the natural polymers, polysaccharides and proteins are preferred due to their solubility, biocompatibility and biodegradability. Self-assembled nanogels from hydrophilic biopolymers, namely pullulan, chitosan and dextran were prepared by attaching hydrophobic moieties such as cholesterol, deoxycholic acid and bile acid to the polymer backbone (Hirakura, Nomura, Aoyama, & Akiyoshi, 2004; Lee & Akiyoshi, 2004; Na, Park, Jo, & Lee, 2006). Daoud-Mahammed et al.

* Corresponding author. Tel.: +91 471 2568 538.
E-mail addresses: sarikapaithal@gmail.com (P.R. Sarika), anilkumarpr@sctimst.ac.in (P.R. Anil Kumar), kdeeps3@gmail.com (D.K. Raj), nirmala@iist.ac.in (N.R. James).

http://dx.doi.org/10.1016/j.carbpol.2014.11.037
0144-8617/

(2007) reported nanoassemblies of lauryl-modified dextran and β-cyclodextrin polymers. Jayakumar and co-workers prepared chitin nanogels by precipitation method and explored the feasibility of using these nanogels for drug delivery to cancer cells, biosensing and bioimaging (Jayakumar, Nair, Rejinold, Maya, & Nair, 2012; Mangalathillam, Rejinold, Nair, Lakshmanan, Nair, & Jayakumar, 2012; Rejinold, Chennazhi, Tamura, Nair, & Rangasamy, 2011).

The present work deals with preparation of cross-linked nanogels from sodium alginate and gelatin. Alginate is a polyanionic and biodegradable polysaccharide composed of β-D-mannuronic acid and α-L-guluronicacid units and is a proven biomedical polymer. Its inert hydrophilic matrix can incorporate drugs, proteins and genes (Li et al., 2013; Maciel et al., 2013). In the presence of divalent cations, alginate forms gels in aqueous medium and these gels are used in drug-delivery applications. Alginate–chitosan nanoparticles have been developed and used as carrier for DNA and for protein delivery exploiting the gelling property of alginate in presence of calcium chloride (Douglas & Tabrizian, 2005; Li, Shi, Du, & Tang, 2007). However, the loss of the cations and the resultant release of the components may pose problems in ionically cross-linked systems. Li et al. (2013) prepared bioreducible alginate-poly(ethylenimine) nanogels through electrostatic interactions and used as an antigen-delivery system. Alginate can also form covalently cross-linked nanogels with hyaluronic acid in polyion complex nanoreactors (De Santis, Diociaiuti, Cametti, & Masci, 2014).

Gelatin, a versatile protein, is being utilized as a drug carrier system because of its appealing physical and chemical properties such as biocompatibility, safety and biodegradability. It is widely used in tissue engineering, gene delivery and wound dressing applications (Kanokpanont, Damrongsakkul, Ratanavaraporn, & Aramwit, 2012; Lim et al., 2011; Tseng et al., 2008). However, poor mechanical properties may limit its potential in certain applications (Boanini, Rubini, Panzavolta, & Bigi, 2010). To overcome this limitation and to improve stability in aqueous medium and mechanical properties, gelatin is subjected to cross-linking by different cross-linking agents (Imani, Rafienia, & Hojjati Emami, 2013; Kim, Jun, Shin, Jang, Kim, & Shin, 2010). Gelatin nanoparticles have been explored and are used for various biomedical applications (Lee, Yhee, Kim, Kwon, & Kim, 2013; Ofokansi, Winter, Fricker, & Coester, 2010; Xu, Gattacceca, & Amiji, 2013). Cross-linking agents such as carbodiimide and glutaraldehyde are being employed for the preparation of cross-linked gelatin nanoparticles (Ethirajan, Schoeller, Musyanovych, Ziener, & Landfester, 2008; Qazvini & Zinatloo, 2011).

Even though gelatin nanogels are prepared by the routes mentioned above, the researchers are interested to develop methods by which the toxic cross-linking agents can be avoided. The latest development in this direction is the preparation of gelatin nanogels using miniemulsion technique by cross-linking of gelatin by genipin, a naturally occurring cross-linking agent for proteins (Choubey & Bajpai, 2010). But, the very high cost of genipin may limit the applicability of the process. Even though reports are available on nanoparticles prepared individually from gelatin and sodium alginate, as mentioned above, the possibility of preparing nanogels by self-cross-linking of these two biopolymers are yet to be investigated. Hence in the present work, we have attempted to prepare alginic aldehyde cross-linked gelatin nanogels using inverse miniemulsion technique. Introduction of aldehyde functionality on alginate and utilizing it for gelatin cross-linking offers a facile route for the preparation of cross-linked AA–gel nanogels. Cross-linking leading to nanogel formation can occur between aldehyde groups in AA and free amino groups in gelatin in the presence of borax (Balakrishnan & Jayakrishnan, 2005). Balakrishnan et al. have developed injectable *in situ* forming alginic aldehyde–gelatin hydrogel scaffolds in this route for wound dressing applications by avoiding extraneous cross-linking agents. In the present work, since the cross-linking takes place in inverse miniemulsion, the process would result in the formation of cross-linked nanogels instead of the macroscopic hydrogels. To the best of our knowledge, this is the first report on cross-linked alginate aldehyde–gelatin nanogels *via* inverse miniemulsion technique. Through this method, we are able to prepare cross-linked nanogels without using any external cross-linking agents. Inverse miniemulsion was prepared by pouring a mixture of AA and gelatin under sonication to the organic phase in which surfactant was dissolved. Physicochemical characterizations of the nanogels were performed by FT-IR spectroscopy, SEM, TEM and DLS. Nontoxic nature of the nanogels was proved by *in vitro* hemocompatibility and cytotoxic studies.

2. Materials and methods

2.1. Materials

Sodium alginate (medium viscosity) and gelatin (Type A) were obtained from Sigma Aldrich, Saint Louis, USA. Sodium metaperiodate, sodium tetra borate (borax), Span 20, sodium chloride, disodium hydrogen phosphate, sodium dihydrogen phosphate, hydroxyl amine hydrochloride, methyl orange, minimum essential medium (MEM), isopropanol, sodium hydroxide, cyclohexane and acetone were obtained from Merk (Mumbai, India). Dialysis tubing (3500 MWCO) was procured from Spectrum Laboratories Inc., CA, USA.

2.2. Methods

2.2.1. Preparation of alginic aldehyde (AA)

Sodium alginate was oxidized to alginic aldehyde by a previously reported procedure (Balakrishnan & Jayakrishnan, 2005). Briefly, into 10 g (0.058 mol) of sodium alginate dissolved in ethanol–water mixture (1:1, v/v), sodium periodate dissolved in minimum amount of water (3.28 g, 0.015 mol, required for 30% oxidation) was added. The reaction mixture was stirred at 20 °C for 6 h in dark. Purification was done by dialysis using dialysis tube of MWCO 3500 for 3 days against distilled water. After the complete removal of periodate, dialysate was frozen and lyophilized. Alginic aldehyde was characterized by FT-IR spectroscopy and the aldehyde content was evaluated by titrimetry (Manju, Muraleedharan, Rajeev, Jayakrishnan, & Joseph, 2011).

2.2.2. Preparation of alginic aldehyde–gelatin (AA–gel) nanogel

Nanogels were prepared by an inverse miniemulsion technique with appropriate modification to the reported procedure (Ethirajan, Schoeller, Musyanovych, Ziener, & Landfester, 2008). A typical procedure for nanogel preparation is as follows. Span 20 (0.2 g) was dissolved in 10 ml of cyclohexane and a mixture of 250 μl of alginic aldehyde (10%, w/v, solution in 0.1 M borax) and 250 μl of gelatin (10%, w/v, solution in water) were added to the solution under sonication over a period of 5 min. The nanogel emulsion was precipitated by drop-wise addition into acetone (50 ml) while stirring with a magnetic stirrer. The precipitate was collected by centrifugation (5000 rpm, for 15 min) and washed three times with water and dried under reduced pressure to obtain the nanogel in powder form. Nanogel samples were prepared with different weight fractions of the water phase and surfactant concentrations to investigate the impact of these factors on the size of the nanogels.

2.3. Characterization

2.3.1. FT-IR spectroscopy

FT-IR spectrum of alginic aldehyde, gelatin and AA–gel nanogels were recorded on a Perkin Elmer FT-IR spectrometer with 32 scans in the scan range of 4000–400 cm^{-1}.

2.3.2. Size and zeta potential measurement

Hydrodynamic diameter and zeta potential of the nanogels were determined by dynamic light scattering (DLS) on a Malvern Zetasizer Nano ZS, UK equipped with a 4 mW He/Ne laser beam operating at $\lambda = 633$ nm. All measurements were performed at 25 °C and each value reported is the average of three series of 10 measurements.

2.3.3. Thermogravimetric analysis (TGA)

Thermal characterization of gelatin, AA and nanogels were performed on Universal V4 7A, TA Instrument with a scanning rate of 10 °C min^{-1} from RT to 800 °C under N_2(g) atmosphere with flow of 20 ml/min.

2.3.4. Morphology analysis by SEM and TEM

Morphology of the nanogel was analyzed by scanning electron microscopy. Lyophilized nanogel powder was redispersed in water (1 mg/ml) by sonication at room temperature and the dispersion was drop cast and dried. It was sputter-coated and analyzed by SEM (FEI Quanta FEG 200 HR Scanning Electron Microscope**)** by applying an acceleration voltage of 10 kV. TEM images were recorded on FEI, TECNAI S twin microscope with an accelerating voltage 300 kV. Sample preparation for TEM was carried out in a similar fashion as that for SEM with a concentration of 1 mg/5 ml. The dispersion was placed on a copper grid and air dried for 2 days before taking the images.

2.3.5. Hemolysis assay

Blood compatibility of the nanogels was evaluated by hemolysis assay using human blood (Morris & Sharma, 2010). The total hemoglobin in the whole blood samples was measured using automatic hematology analyzer (Sysmex-K 4500). Briefly, 0.9 ml of anticoagulated fresh human blood was added to 0.1 ml of PBS containing different concentrations of nanogels (0.2, 0.4, 0.6, 0.8, 1 mg/ml). PBS and 0.1% of Na_2CO_3 were used as negative (0% hemolysis) and positive controls (100% hemolysis) respectively. All samples were incubated at 37 °C for 90 min. After incubation, samples were centrifuged at 4500 rpm for 15 min to obtain the plasma. Optical density of the hemoglobin in plasma was analyzed spectrophotometrically and it was calculated by the following equation:

$$\text{Plasma Hb} = \frac{2[A_{415} - (A_{380} + A_{450})] \times 1000 \times \text{dilution factor}}{E \times 1.655} \quad (1)$$

where A_{415} denotes the Soret band based absorption of hemoglobin. A_{380} and A_{450} stands for correction factors applied for uroporphyrin absorption falling in the same wavelength range. E represents the molar absorptivity value of oxyhemoglobin at 415 nm and is 79.46. The correction factor for accounting the turbidity of plasma sample is 1.655. Hemolysis % was calculated by

$$\%\,\text{Hemolysis} = \frac{\text{Plasma Hb value of the sample}}{\text{Total Hb value of blood}} \times 100 \quad (2)$$

2.3.6. Blood coagulation studies using PTT

Blood-coagulating effect of AA–gel nanogels was analyzed by partial thromboplastin time (PTT) (ISO 10993-4:2002 (E)). Blood from human volunteer was collected into the anticoagulant, ACD (acid citrate dextrose). Nanogel (1 mg) was dispersed in 1 ml of PBS and 1.8 ml of the blood was treated with 200 μl of the sample. One milliliter of blood was immediately taken for initial analysis and remaining blood was incubated with the samples for 30 min under agitation at 70 ± 5 rpm using an Environ shaker thermostated at 35 ± 2 °C (WPTRU012). Three polystyrene culture dishes with PBS were exposed to blood (1.8 ml of blood and 200 μl of PBS) as reference. After incubation, blood samples were centrifuged at 4000 rpm for 15 min and platelet poor plasma was aspirated.

Partial thromboplastin time in each sample was detected using a reagent kit obtained from Diagnostica Stago (France) on Start 4, coagulation analyzer. Estimations were performed in triplicate.

2.3.7. Cytotoxicity studies

In vitro cytotoxicity of AA–gel nanogels were analyzed by MTT assay using MCF-7 cancer cells. We selected MCF-7 cell line for the cytotoxicity analysis since the AA–gel nanogels are designed for drug-delivery application towards breast cancer cells. MCF-7 (Breast cancer cell line, NCCS Pune) was seeded on a 96-well plate with a density of 5000 cells/well. MTT assay is a colorimetric assay for evaluating the metabolic activity of cells based on their ability to reduce the tetrazolium component of MTT into purple-colored formazan crystals. Four different concentrations of nanogels (0.125, 0.25, 0.5 and 1 mg/ml) were prepared by dilution with the 2× culture medium containing serum. When the cells reached subconfluency, equal volume (100 μl) of different concentrations of the nanogels, extract of negative control (ultra-high-molecular-weight polyethylene), positive control (dilute phenol) and cell control (cells cultured in normal medium) were added and incubated for a period of 24 h at 37 °C. After incubation, extract and control medium were replaced with 50 μl MTT solution (1 mg/ml without supplements) and incubated for 2 h. After discarding the MTT solutions, 100 μl of isopropanol was added to all wells and swayed the plates. The color developed was quantified by measuring absorbance at 570 nm using spectrophotometer.

2.3.8. LDH assay

Cell death or cytotoxicity is classically evaluated by the quantification of plasma membrane damage. Lactate dehydrogenase (LDH) is a stable cytoplasmic enzyme present in all cells and is rapidly released into the cell culture supernatant upon membrane damage or cell lysis. The amount of released LDH is proportional to the number of damaged cells. LDH detection kit (Xenometrix four parameter detection kit) was used to measure the LDH activity. This assay is a fast and simple method to determine changes in the plasma membrane upon incubation with the sample. This version of the LDH test is unaffected by pyruvate present in the medium. LDH reduces pyruvate to lactate by oxidizing NADH to NAD+:

$$Pyruvate + NADH + H^+ \xrightarrow{LDH} Lactate + NAD^+$$

The consumption of NADH is measured spectrophotometrically by a decrease in the OD at 340 nm.

For LDH experiments, MCF-7 (Breast cancer cell line, NCCS Pune) cells were seeded on a 96-well plate with a density of 5000 cells/well and incubated at 37 °C for 24 h. After 24 h of incubation, the media was removed and replaced with 100 μl of fresh media containing different concentrations of AA–gel nanogels (0.125, 0.25, 0.5 and 1 mg/ml) and incubated for 24 h. After the incubation, the 96-well plate was centrifuged at 3000 rpm for 10 min to obtain the supernatant and 10 μl of supernatant from each well was added to 120 μl of the reconstituted LDH solution. Absorbance of the solution was measured on a microplate reader (Biotek, USA) at 380 nm for 1 h at an interval of 10 min. For this assay, Triton-X (1%)-treated cells were used as positive control and cells cultured in normal medium were used as negative control.

3. Results and discussion

3.1. Preparation of nanogels

Alginic aldehyde–gelatin hydrogels have been reported in the literature for various biomedical applications. Jayakrishnan and co-workers have reported the efficacy of in situ forming alginic aldehyde–gelatin hydrogels for wound healing, as an injectable drug-delivery vehicle and as sealant for polyester vascular graft (Balakrishnan & Jayakrishnan, 2005; Balakrishnan, Mohanty, Umashankar, & Jayakrishnan, 2005; Manju, Muraleedharan, Rajeev, Jayakrishnan, & Joseph, 2011). Recently, Sarker et al. (2014) reported the development of alginic aldehyde–gelatin hydrogel microcapsules for tissue engineering. The application of alginic aldehyde–gelatin hydrogels for myocardial infarction repair has been demonstrated recently (Bai et al., 2013). Even though alginic aldehyde–gelatin hydrogels have been extensively investigated for various applications, reports are not found on its nanoscopic counterparts. The main objective of the current study is to prepare nanoscale alginic aldehyde–gelatin hydrogels. An inverse miniemulsion technique is adopted for preparing cross-linked AA–gel nanogels. These nanoscopic counterparts are formed by an inverse miniemulsion process involving Schiff's base reaction between aldehyde groups and $-NH_2$ groups. Aldehyde functionality was introduced on sodium alginate by periodate oxidation for cross-linking with $-NH_2$ groups of gelatin. Periodate cleaves the vicinal diols present in the polysaccharide resulting in dialdehyde functionalities. The FT-IR spectra of AA and sodium alginate are shown in Fig. 1B. In the spectrum of AA, a characteristic aldehyde peak at 1746 cm^{-1} is seen which is not present in the spectrum of sodium alginate (Fig. 1A), there by confirming the oxidation. Aldehyde content in AA was estimated by titrimetry and was found to be 5.5×10^{-3} mol/g.

Nanogels were prepared through inverse miniemulsion process (Scheme 1). According to Landfester, Willert, and Antonietti (2000), an inverse miniemulsion contains hydrophilic droplets as dispersed phase in hydrocarbon solution of surfactant as the continuous phase. In the present work, cyclohexane was used as continuous phase, Span 20 as surfactant and aqueous mixture of AA and gelatin as non continuous phase. AA with 30% oxidation was selected for the reaction, because sufficient aldehyde content is required for the cross-linking. AA solution (10% solution, w/v) was prepared in 0.1 M

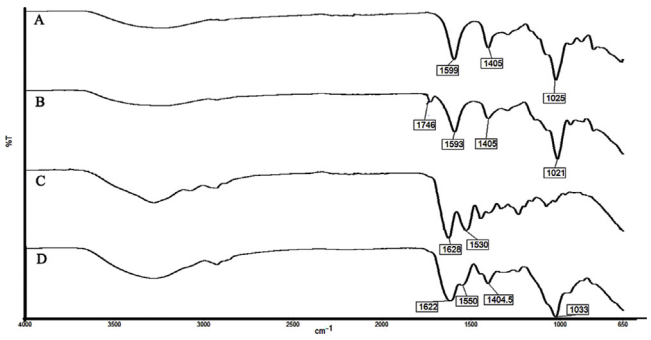

Fig. 1. FT-IR spectrum of sodium alginate (A), 30% oxidized alginic aldehyde (B), gelatin (C) and AA–gel nanogel (D). In the spectrum of AA, a new peak at 1746 cm^{-1} corresponds to aldehyde functionality.

borax which provided alkaline pH. The hydroxyl groups of AA complexes with borate which was formed by the dissociation of borax in aqueous medium (Strauss & Kral, 1982). If gelatin is added to this AA–borax complex, Schiff's base reaction occurs between aldehyde groups of AA and amino groups of gelatin and macroscopic hydrogel would be formed in less than 1 min (Balakrishnan & Jayakrishnan, 2005). Therefore, in the present work, the mixture was added to surfactant containing cyclohexane before it formed hydrogel and sonicated for 5 min to obtain inverse miniemulsion. Inverse miniemulsion was formed when the aqueous AA–gel mixture was dispersed in continuous cyclohexane phase. Ultrasonication was selected for the dispersion, since it is a very efficient method to reduce the size of the droplets. Initially, polydispersity of the AA–gel droplets would be high, later during ultrasonication, polydispersity would decrease due to constant fusion and fission process (Landfester, 2006). Span 20, the surfactant dissolved in cyclohexane stabilizes the resultant AA–gel droplets from growth by collision, coalescence and Ostwald ripening. Cross-linked AA–gel nanoparticles were formed inside the surfactant micelle.

The size of the nanogel can be tuned by modulating certain parameters. Landfester, Bechthold, Tiarks, and Antonietti (1999) reported that the amount of surfactant determines the droplet area and hence the particle size at constant ultrasonication time. We investigated the impact of surfactant/water ratio on the particle size by changing the surfactant to water weight percentage at constant ultrasonication time and amplitude. The particle size

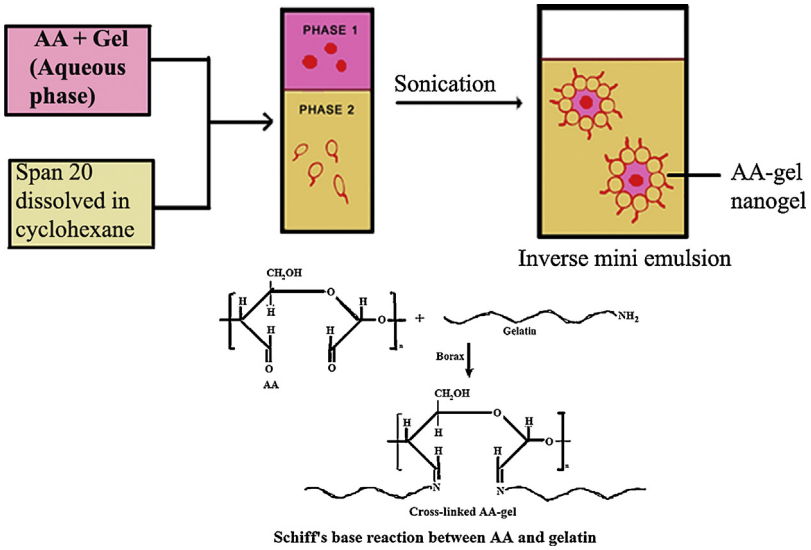

Scheme 1. Formation of inverse miniemulsion from AA and gel. Cross-linking occurs due to Schiff's base reaction between aldehyde groups of AA and amino groups of gelatin.

Table 1
Effect of volume of aqueous phase and concentration of surfactant on size of the nanogel particles.

Amount of surfactant with respect to organic phase (wt %)	Total volume of aqueous phase (μl)	Volume of organic phase (ml)	Size (nm) of nanogel in cyclohexane
1	250	10	193 ± 8
1	500	10	240 ± 9
1	750	10	256 ± 7
2	250	10	127 ± 6
2	500	10	168 ± 9
2	750	10	235 ± 5
3	250	10	103 ± 8
3	500	10	172 ± 9
3	750	10	200 ± 7

With increase in concentration of surfactant, particle size decreases and increases with increase in volume of the aqueous phase.

of the nanogels can be varied over a wide range by changing the amount of the surfactant. From Table 1, it is clear that when surfactant concentration was increased, keeping the volume of aqueous phase constant, the size of the nanogel particles decreased. Initially, the surfactant Span 20 dissolved in cyclohexane, self-assembled to micelle and when the aqueous AA–gel mixture was added to cyclohexane and agitated by sonication, droplets of AA–gel were formed. Then the nanosized droplets get engulfed by the surfactant micelle and stabilize the nanogel droplets from coalescence and Ostwald ripening. Small droplets undergo very fast collision and if the surfactant amount was less (1% with respect to the organic phase), the stabilization was decreased, and droplets combined to a big droplet resulting in increased particle size. When the concentration of surfactant increased to 3%, the particle size was again decreased because more amount of surfactant was there to stabilize the small droplets.

Parameters such as the volume of the aqueous phase and AA–gel weight ratio also have an impact on the size of the alginate AA–gel nanogels. Impact of the volume of aqueous phase (AA and gelatin) in the emulsion on the size of the nanogel particles was investigated by maintaining constant surfactant concentration against the aqueous phase to ensure that the same amount of surfactant surrounded the water droplets. Total volume of aqueous phase was varied from 250 to 750 μl by keeping the organic phase volume as 10 ml. The size of the nanogel particles was analyzed by DLS and is shown in Table 1. From the table, it can be seen that the size of the nanogels increased with increase in volume of aqueous phase when surfactant concentration was kept constant.

The influence of weight ratio of AA and gelatin was also examined. For these studies, surfactant concentration was fixed as 2% with respect to the organic phase. The particle size was measured by varying the volume of AA and gelatin, while keeping the total volume of aqueous phase as 500 μl. Table 2 shows the results of the particle size measurements. From Table 2, it is clear that with increase in volume of AA, the size of the nanogel was decreased. With increase in the volume of AA, aldehyde functionality available for cross-linking was increased and due to the enhanced cross-linking, the size of the nanogel was decreased. Greater extent of cross-linking was also evident from the size of the redispersed nanogels in aqueous medium. Nanogels cross-linked to higher extent show lower size. Even though the combination with surfactant amount of 3% gave nanogels with very small size, the combination which resulted in the smallest nanogels with medium amount of surfactant (surfactant concentration 2%) with a total volume of aqueous phase as 500 μl (250 μl of gelatin and 250 μl of AA) and size 168 ± 9 nm was selected for further studies.

Nanogel particles were isolated by precipitation of the inverse emulsion in acetone, followed by centrifugation. The particles were washed many times with water to remove the impurities and surfactants and finally dried under reduced pressure to obtain nanogel in powder form. These chemically cross-linked AA–gel nanogels thus obtained could be redispersed in water without the use of additional surfactant, since AA contain carboxylic acid groups which provide negative zeta potential to stabilize the nanoparticles. The particle size of the water-redispersed nanogels was measured by DLS and was found to be 297 ± 6 nm. The redispersed nanogels showed a zeta potential of −36.9 mV indicating good stability of the nanogels. Negative surface charge of the AA–gel nanogels is due to the charge density of AA at neutral pH since at this pH, all the acid groups in AA remain deprotonated. Gessner, Waicz, Lieske, Paulke, Mäder, and Müller (2000) reported that nanoparticles with a positive surface charge or hydrophobic surface promotes protein adsorption and fast reticuloendothelial clearance (REF). Negatively charged AA-gel nanogels may avoid protein adsorption and REF clearance and can provide long circulation time and maximum EPR effect. In an aqueous medium, the hydrodynamic radius of AA–gel nanogel is much larger than that in organic solvent, as more water can diffuse into the polymer network of both AA and gelatin from the dispersion medium to occupy the channels or to the free volume in between the polymer strands until it become fully swollen.

3.2. Characterization by FT-IR and TGA

FT-IR spectra of the dried nanogel (Fig. 1D) powder samples were recorded in the range of 400–4000 cm^{-1}. Absorption bands from both gelatin and AA are seen in the spectrum. Aldehyde peak at 1746 cm^{-1} is not seen in the spectrum of nanogel, indicating the cross-linking between AA and gelatin (Fig. 1C). The peak at

Table 2
Effect of weight fraction of AA and gel on size of the nanogels.

Sample code	Amount of surfactant with respect to organic phase volume (wt %)	Total volume of aqueous phase (μl)	Volume of organic phase (ml)	Size (nm) in cyclohexane	Size of water dispersed nanogels (nm)
AA–gel	2	100(AA) + 400(gel)	10	210 ± 5	1290 ± 6
AA–gel	2	200(AA) + 300(gel)	10	206 ± 6	900 ± 7
AA–gel	2	250(AA) + 250(gel)	10	168 ± 9	297 ± 6
AA–gel	2	300(AA) + 200(gel)	10	177 ± 8	657 ± 5
AA–gel	2	400(AA) + 100(gel)	10	170 ± 5	376 ± 2

With increase in concentration of AA, cross-linking increases and particle size decreases.

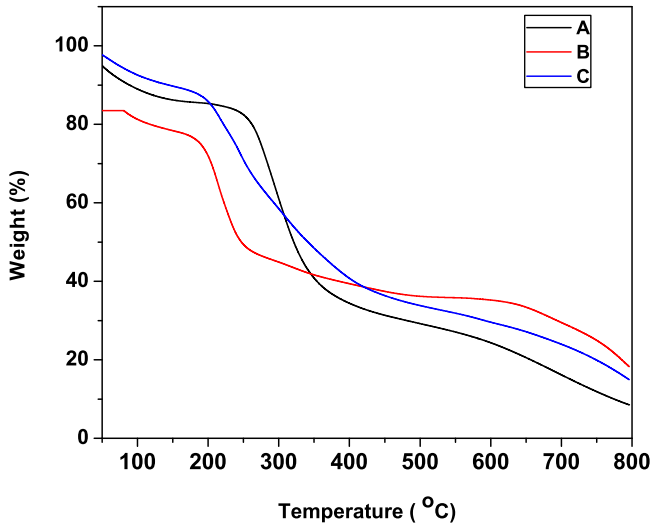

Fig. 2. TGA curves of gelatin (A), AA (B) and AA–gel nanogel (C).

1622 cm^{-1} corresponds to the —C═N group (Schiff's base) formed between aldehyde and amino groups (Issa, Khedr, & Rizk, 2008; Ye, Xiong, & Sun, 2012). This —C═N band is broad due to the overlap of amide | band at 1628 cm^{-1} of gelatin. Amide ‖ band at 1530 cm^{-1} of gelatin is shifted to 1550 cm^{-1} in nanogel and confirms the involvement of amino group in Schiff's base formation (Sarker et al., 2014). The peak observed at 1033 cm^{-1} in the spectrum of nanogel corresponds to AA. All these observations confirm the formation of cross-linked nanogels.

TGA curves of AA, gelatin and nanogel are shown in Fig. 2. The first degradation step of AA (Fig. 2B) occurs in the range of 50–100 °C, which corresponds to the elimination of absorbed and bound water from AA. The second degradation step due to the structural degradation of the main chain starts at 250 °C. Gelatin also exhibits three degradation steps (Fig. 2A). First step corresponds to elimination of water in the region of 50–100 °C and the second and third steps are due to the breakage of protein chain and peptide bond rupture (Cai & Kim, 2010). It can be seen from the thermograms that the nanogel (Fig. 2C) shows a significantly different thermal behavior. Thermal stability of the nanogel is lower than that of gelatin, but higher than that of AA. The thermal stability of AA–gel nanogels has been increased due to the cross-linking.

3.3. Morphology analysis by SEM and TEM

Morphology of the nanogels as obtained in inverse miniemulsion and after redispersion in water were analyzed by SEM and TEM. Fig. 3A shows the SEM image of as-obtained nanogels formed in the miniemulsion. All the particles have a spherical morphology with a smooth surface and diameter of about 120–147 nm. The size of the nanogels observed by SEM was less than those measured using DLS. The variation in the particle size between SEM and DLS measurements is due to the difference in the processing. In DLS, particle size analysis was performed in solution and the size obtained is the hydrodynamic diameter, whereas SEM analysis was performed on the dried particles.

Morphology of the redispersed particles was also analyzed by SEM and TEM to investigate the change in size and shape due to redispersion in water. Fig. 3B and C shows, respectively, the SEM and TEM images of the redispersed particles after drying. Redispersed nanogels show an average size of 200 nm. On redispersion in water, slight increase in size was observed due to the swelling of the nanogels and was found to be 297 nm by DLS measurement.

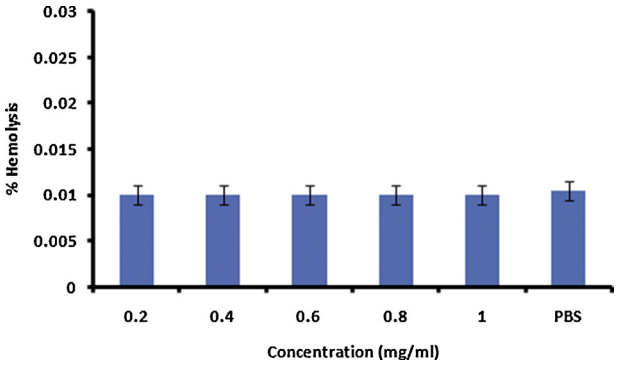

Fig. 4. Hemolysis assay of nanogels with different concentrations from 0.2 to 1 mg/ml in PBS. Positive control, Na_2CO_3 (0.1%) shows 100% hemolysis, which is not included in the graph.

3.4. Hemolysis assay

Hemolysis test was conducted to study the compatibility of nanogels with blood cells since these particles are designed for drug-delivery applications. Nanogels interact with a large fraction of blood cells in the blood prior to distribution into tissues. Nanogels should possess long-term stability and minimum interaction with blood components in the bloodstream. Fig. 4 shows the hemolytic potential of various concentrations of nanogels. It can be seen that % hemolysis is far below 5%, the critical safe hemolytic ratio for biomaterials according to ISO/TR 7406.

Plasma coagulation assay using PTT measurement was employed to analyze the plasma coagulating effect of AA–gel nanogels. Average % change in PTT in plasma for samples (1 mg/ml) and reference after 30 min exposure was 2.18 ± 0.06 and 1.96 ± 0.4, respectively. The data indicate that exposure of samples to blood

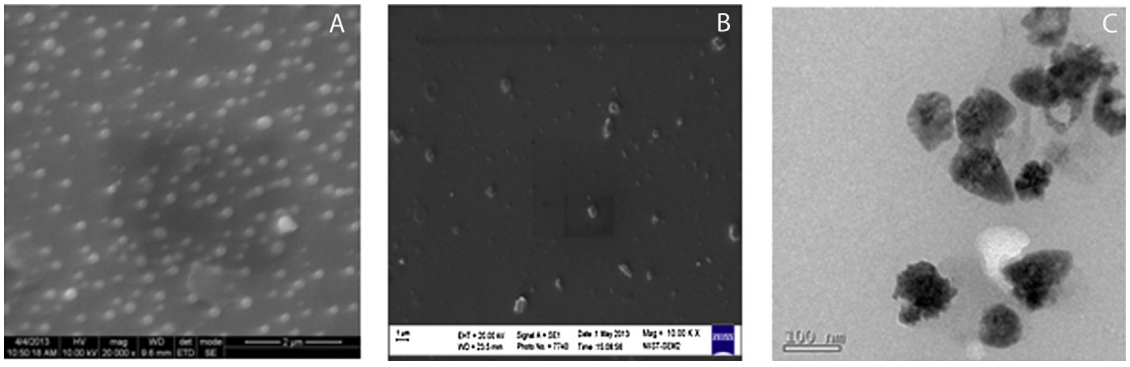

Fig. 3. SEM image of nanogels as formed in miniemulsion (A), SEM and TEM images of the particles, after redispersion in aqueous medium (B, C).

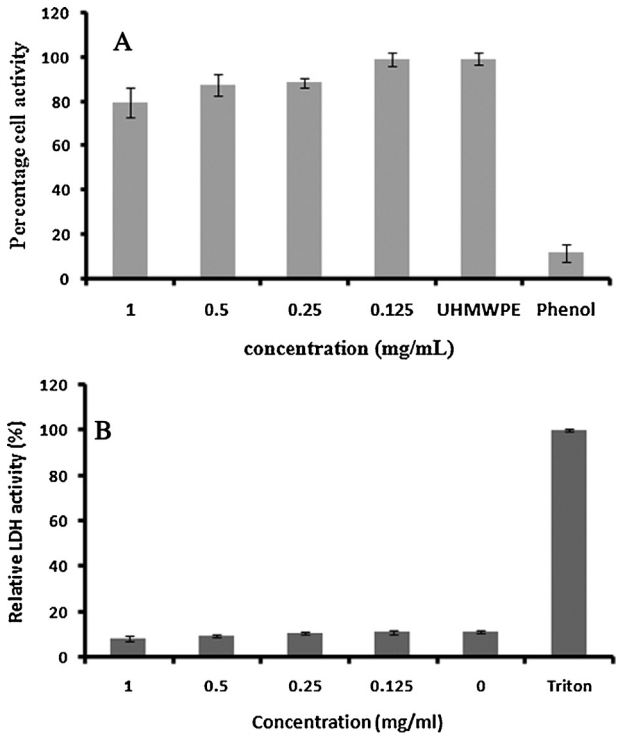

Fig. 5. MTT assay (A) and LDH assay (B) of AA–gel nanogels on MCF-7 cells. MTT and LDH assay proved the nontoxicity of nanogels.

does not have any effect on PTT. Thus, the percentage hemolysis study and PTT measurements indicated that these nanogel samples are hemocompatible.

3.5. Cytotoxicity studies

3.5.1. MTT assay

For biomedical applications, it is necessary to evaluate the toxicity of the materials. MTT assay was performed to evaluate cytotoxicity of AA–gel nanogels towards MCF-7 cancer cell lines for four different concentrations ranging from 0.125 to 1 mg/ml. Fig. 5a shows the viability of cells treated with different concentrations of nanogels for 24 h in comparison with those treated with phenol and UHMWPE. From the results, it is evident that more than 80% cells cultured with nanogels remained viable in all the four concentrations. There is no significant cytotoxicity in any of the selected concentrations.

3.5.2. LDH assay

The *in vitro* cytotoxicity of AA–gel nanogels towards MCF-7 cancer cell lines cells was further evaluated by LDH assay. Cytotoxic agents damage cell membrane and cause rupture leading to release of LDH into the extracellular medium. Estimation of released LDH can be used to analyze cytocompatibility of the nanogel. As shown in Fig. 5b, the LDH release of MCF-7 cells treated with AA–gel nanogel was lower than that of the cell control at all test concentrations. The result indicates noncytotoxicity of the nanogels.

4. Conclusion

The main aim of this work was to prepare nanosized alginic aldehyde–gelatin nanogels. Cross-linked nanogels were prepared by an inverse miniemulsion process. Properties of the nanogels were analyzed by SEM, TEM, DLS, FT-IR and TGA. Nanogel powder could be redispersed in water without the use of additional surfactant and the particles exhibited spherical morphology. This was possible due to the high negative zeta potential possessed by these nanoparticles. Cytocompatibility and hemocompatibility of the nanogels suggest that this nanogel system is a potential candidate for various biomedical applications including drug delivery.

Acknowledgements

The authors thank the Director, IIST, for the financial support and the Director, SCTIMST, for cytotoxicity and hemocompatibility studies. We also thank SAIF, IIT Madras, for SEM analysis, the Director, NIIST, Thiruvananthapuram, for TEM analysis.

References

Bai, X., Fang, R., Zhang, S., Shi, X., Wang, Z., Chen, X., Yang, J., Hou, X., Nie, Y., & Li, Y. (2013). Self-cross-linkable hydrogels composed of partially oxidized alginate and gelatin for myocardial infarction repair. *Journal of Bioactive and Compatible Polymers*, *28*(2), 126–140.

Balakrishnan, B., & Jayakrishnan, A. (2005). Self-cross-linking biopolymers as injectable *in situ* forming biodegradable scaffolds. *Biomaterials*, *26*(18), 3941–3951.

Balakrishnan, B., Mohanty, M., Umashankar, P., & Jayakrishnan, A. (2005). Evaluation of an in situ forming hydrogel wound dressing based on oxidized alginate and gelatin. *Biomaterials*, *26*(32), 6335–6342.

Boanini, E., Rubini, K., Panzavolta, S., & Bigi, A. (2010). Chemico-physical characterization of gelatin films modified with oxidized alginate. *Acta Biomaterialia*, *6*(2), 383–388.

Cai, Z., & Kim, J. (2010). Preparation and characterization of novel bacterial cellulose/gelatin scaffold for tissue regeneration using bacterial cellulose hydrogel. *Journal of Nanotechnology in Engineering and Medicine*, *1*(2), 021002.

Choubey, J., & Bajpai, A. (2010). Investigation on magnetically controlled delivery of doxorubicin from superparamagnetic nanocarriers of gelatin crosslinked with genipin. *Journal of Materials Science: Materials in Medicine*, *21*(5), 1573–1586.

Daoud-Mahammed, S., Couvreur, P., Bouchemal, K., Chéron, M., Lebas, G., Amiel, C., & Gref, R. (2009). Cyclodextrin and polysaccharide-based nanogels: entrapment of two hydrophobic molecules, benzophenone and tamoxifen. *Biomacromolecules*, *10*(3), 547–554.

Daoud-Mahammed, S., Ringard-Lefebvre, C., Razzouq, N., Rosilio, V., Gillet, B., Couvreur, P., Amiel, C., & Gref, R. (2007). Spontaneous association of hydrophobized dextran and poly-β-cyclodextrin into nanoassemblies: Formation and interaction with a hydrophobic drug. *Journal of Colloid and Interface Science*, *307*(1), 83–93.

De Santis, S., Diociaiuti, M., Cametti, C., & Masci, G. (2014). Hyaluronic acid and alginate covalent nanogels by template cross-linking in polyion complex micelle nanoreactors. *Carbohydrate Polymers*, *101*, 96–103.

Douglas, K. L., & Tabrizian, M. (2005). Effect of experimental parameters on the formation of alginate–chitosan nanoparticles and evaluation of their potential application as DNA carrier. *Journal of Biomaterials Science, Polymer Edition*, *16*(1), 43–56.

Ethirajan, A., Schoeller, K., Musyanovych, A., Ziener, U., & Landfester, K. (2008). Synthesis and optimization of gelatin nanoparticles using the miniemulsion process. *Biomacromolecules*, *9*(9), 2383–2389.

Gessner, A., Waicz, R., Lieske, A., Paulke, B.-R., Mäder, K., & Müller, R. (2000). Nanoparticles with decreasing surface hydrophobicities: influence on plasma protein adsorption. *International Journal of Pharmaceutics*, *196*(2), 245–249.

Hirakura, T., Nomura, Y., Aoyama, Y., & Akiyoshi, K. (2004). Photoresponsive nanogels formed by the self-assembly of spiropyrane-bearing pullulan that act as artificial molecular chaperones. *Biomacromolecules*, *5*(5), 1804–1809.

Imani, R., Rafienia, M., & Hojjati Emami, S. (2013). Synthesis and characterization of glutaraldehyde-based crosslinked gelatin as a local hemostat sponge in surgery: An *in vitro* study. *Bio-medical Materials and Engineering*, *23*(3), 211–224.

Issa, R. M., Khedr, A. M., & Rizk, H. (2008). ^{1}H NMR, IR and UV/VIS spectroscopic studies of some schiff bases derived from 2-aminobenzothiazole and 2-amino-3-hydroxypyridine. *Journal of the Chinese Chemical Society*, *55*(4), 875–884.

Jayakumar, R., Nair, A., Rejinold, N. S., Maya, S., & Nair, S. (2012). Doxorubicin-loaded pH-responsive chitin nanogels for drug delivery to cancer cells. *Carbohydrate Polymers*, *87*(3), 2352–2356.

Kabanov, A. V., & Vinogradov, S. V. (2009). Nanogels as pharmaceutical carriers: finite networks of infinite capabilities. *Angewandte Chemie International Edition*, *48*(30), 5418–5429.

Kanokpanont, S., Damrongsakkul, S., Ratanavaraporn, J., & Aramwit, P. (2012). An innovative bi-layered wound dressing made of silk and gelatin for accelerated wound healing. *International Journal of Pharmaceutics*, *436*(1), 141–153.

Kim, M. S., Jun, I., Shin, Y. M., Jang, W., Kim, S. I., & Shin, H. (2010). The development of genipin-crosslinked poly(caprolactone) (PCL)/gelatin nanofibers for tissue engineering applications. *Macromolecular Bioscience*, *10*(1), 91–100.

Landfester, K. (2006). Synthesis of colloidal particles in miniemulsions. *Annual Review of Material Research*, *36*, 231–279.

Landfester, K., Bechthold, N., Tiarks, F., & Antonietti, M. (1999). Formulation and stability mechanisms of polymerizable miniemulsions. *Macromolecules*, *32*(16), 5222–5228.

Landfester, K., Willert, M., & Antonietti, M. (2000). Preparation of polymer particles in nonaqueous direct and inverse miniemulsions. *Macromolecules*, *33*(7), 2370–2376.

Lee, I., & Akiyoshi, K. (2004). Single molecular mechanics of a cholesterol-bearing pullulan nanogel at the hydrophobic interfaces. *Biomaterials*, *25*(15), 2911–2918.

Lee, S. J., Yhee, J. Y., Kim, S. H., Kwon, I. C., & Kim, K. (2013). Biocompatible gelatin nanoparticles for tumor-targeted delivery of polymerized siRNA in tumor-bearing mice. *Journal of Controlled Release*, *172*(1), 358–366.

Li, P., Luo, Z., Liu, P., Gao, N., Zhang, Y., Pan, H., Liu, L., Wang, C., Cai, L., & Ma, Y. (2013). Bioreducible alginate-poly (ethylenimine) nanogels as an antigen-delivery system robustly enhance vaccine-elicited humoral and cellular immune responses. *Journal of Controlled Release*, *168*(3), 271–279.

Li, T., Shi, X. W., Du, Y. M., & Tang, Y. F. (2007). Quaternized chitosan/alginate nanoparticles for protein delivery. *Journal of Biomedical Materials Research Part A*, *83*(2), 383–390.

Lim, Y. C., Johnson, J., Fei, Z., Wu, Y., Farson, D. F., Lannutti, J. J., Choi, H. W., & Lee, L. J. (2011). Micropatterning and characterization of electrospun poly ((-caprolactone)/gelatin nanofiber tissue scaffolds by femtosecond laser ablation for tissue engineering applications. *Biotechnology and Bioengineering*, *108*(1), 116–126.

Maciel, D., Figueira, P., Xiao, S., Hu, D., Shi, X., Rodrigues, J., Tomás, H., & Li, Y. (2013). Redox-responsive alginate nanogels with enhanced anticancer cytotoxicity. *Biomacromolecules*, *14*(9), 3140–3146.

Mangalathillam, S., Rejinold, N. S., Nair, A., Lakshmanan, V.-K., Nair, S. V., & Jayakumar, R. (2012). Curcumin loaded chitin nanogels for skin cancer treatment via the transdermal route. *Nanoscale*, *4*(1), 239–250.

Manju, S., Muraleedharan, C. V., Rajeev, A., Jayakrishnan, A., & Joseph, R. (2011). Evaluation of alginate dialdehyde cross-linked gelatin hydrogel as a biodegradable sealant for polyester vascular graft. *Journal of Biomedical Materials Research Part B: Applied Biomaterials*, *98*(1), 139–149.

Morris, V. B., & Sharma, C. P. (2010). Folate mediated *in vitro* targeting of depolymerised trimethylated chitosan having arginine functionality. *Journal of Colloid and Interface Science*, *348*(2), 360–368.

Munshi, N., De, T. K., & Maitra, A. (1997). Size modulation of polymeric nanoparticles under controlled dynamics of microemulsion droplets. *Journal of Colloid and Interface Science*, *190*(2), 387–391.

Na, K., Park, K. M., Jo, E. A., & Lee, K. S. (2006). Self-organized pullulan/deoxycholic acid nanogels: Physicochemical characterization and anti-cancer drug-releasing behavior. *Biotechnology and Bioprocess Engineering*, *11*(3), 262–267.

Nesamony, J., & Kolling, W. M. (2005). IPM/DOSS/water microemulsions as reactors for silver sulfadiazine nanocrystal synthesis. *Journal of Pharmaceutical Sciences*, *94*(6), 1310–1320.

Nesamony, J., Singh, P. R., Nada, S. E., Shah, Z. A., & Kolling, W. M. (2012). Calcium alginate nanoparticles synthesized through a novel interfacial cross-linking method as a potential protein drug delivery system. *Journal of Pharmaceutical Sciences*, *101*(6), 2177–2184.

Ofokansi, K., Winter, G., Fricker, G., & Coester, C. (2010). Matrix-loaded biodegradable gelatin nanoparticles as new approach to improve drug loading and delivery. *European Journal of Pharmaceutics and Biopharmaceutics*, *76*(1), 1–9.

Oh, J. K., Drumright, R., Siegwart, D. J., & Matyjaszewski, K. (2008). The development of microgels/nanogels for drug delivery applications. *Progress in Polymer Science*, *33*(4), 448–477.

Oh, J. K., Lee, D. I., & Park, J. M. (2009). Biopolymer-based microgels/nanogels for drug delivery applications. *Progress in Polymer Science*, *34*(12), 1261–1282.

Pileni, M. (1997). Nanosized particles made in colloidal assemblies. *Langmuir*, *13*(13), 3266–3276.

Qazvini, N. T., & Zinatloo, S. (2011). Synthesis and characterization of gelatin nanoparticles using CDI/NHS as a non-toxic cross-linking system. *Journal of Materials Science: Materials in Medicine*, *22*(1), 63–69.

Raemdonck, K., Demeester, J., & De Smedt, S. (2009). Advanced nanogel engineering for drug delivery. *Soft Matter*, *5*(4), 707–715.

Rejinold, N. S., Chennazhi, K. P., Tamura, H., Nair, S. V., & Rangasamy, J. (2011). Multifunctional chitin nanogels for simultaneous drug delivery, bioimaging, and biosensing. *ACS Applied Materials & Interfaces*, *3*(9), 3654–3665.

Rejinold, N. S., Nair, A., Sabitha, M., Chennazhi, K., Tamura, H., Nair, S. V., & Jayakumar, R. (2012). Synthesis, characterization and *in vitro* cytocompatibility studies of chitin nanogels for biomedical applications. *Carbohydrate Polymers*, *87*(1), 943–949.

Sarker, B., Papageorgiou, D. G., Silva, R., Zehnder, T., Gul-E-Noor, F., Bertmer, M., Kaschta, J., Chrissafis, K., Detsch, R., & Boccaccini, A. R. (2014). Fabrication of alginate–gelatin crosslinked hydrogel microcapsules and evaluation of the microstructure and physico-chemical properties. *Journal of Materials Chemistry B*.

Sasaki, Y., Asayama, W., Niwa, T., Sawada, S. i., Ueda, T., Taguchi, H., & Akiyoshi, K. (2011). Amphiphilic polysaccharide nanogels as artificial chaperones in cell-free protein synthesis. *Macromolecular Bioscience*, *11*(6), 814–820.

Sato, H., Ohtsu, T., & Komasawa, I. (2000). Atomic force microscopy study of ultrafine particles prepared in reverse micelles. *Journal of Colloid and Interface Science*, *230*(1), 200–204.

Shah, P. P., Desai, P. R., Patel, A. R., & Singh, M. S. (2012). Skin permeating nanogel for the cutaneous co-delivery of two anti-inflammatory drugs. *Biomaterials*, *33*(5), 1607–1617.

Sims, J., Kumbhar, A., Lin, J., Agnoli, F., Carpenter, E., Sangregorio, C., Frommen, C., Kolesnichenko, V., & O'Connor, C. (2002). Synthesis and manipulation of nanophase magnetic materials. *Molecular Crystals and Liquid Crystals*, *379*(1), 113–120.

Strauss, G., & Kral, F. (1982). Borate complexes of amphotericin B: Polymeric species and aggregates in aqueous solutions. *Biopolymers*, *21*(2), 459–470.

Tseng, C.-L., Wu, S. Y.-H., Wang, W.-H., Peng, C.-L., Lin, F.-H., Lin, C.-C., Young, T.-H., & Shieh, M.-J. (2008). Targeting efficiency and biodistribution of biotinylated-EGF-conjugated gelatin nanoparticles administered via aerosol delivery in nude mice with lung cancer. *Biomaterials*, *29*(20), 3014–3022.

Xu, J., Gattacceca, F., & Amiji, M. (2013). Biodistribution and pharmacokinetics of EGFR-targeted thiolated gelatin nanoparticles following systemic administration in pancreatic tumor-bearing mice. *Molecular Pharmaceutics*, *10*(5), 2031–2044.

Ye, J., Xiong, J., & Sun, R. (2012). The fluorescence property of Schiff's bases of carboxymethyl cellulose. *Carbohydrate Polymers*, *88*(4), 1420–1424.